HYDROKINETIC TURBINE DESIGN AND ANALYSIS FOR INDIAN RIVERS

A Graduate Project Report submitted to Manipal Academy of Higher Education in partial fulfilment of the requirements for the award of the degree of

BACHELOR OF TECHNOLOGY

in

Mechanical Engineering

by

STUDENT NAME	REG. NO.	EMAIL ID	CONTACT NO.
Abhishek Nain	170909318	abhishek.nain@learner.manipal.edu	8209330377
Dipayan Maji	170909228	dipayan.maji@learner.manipal.edu	9650500290
Krishnakanth Mohanta	170909082	krishnakanth.mohanta@manipal.edu	7974756690

under the guidance of

Prof. Jayakrishnan Radhakrishnan, Assistant Professor – Senior Scale
Department of Aeronautical and Automobile Engineering
Contact Number: + 91 89702 21602
Email Id: jayakrishnan.r@manipal.edu

Prof. Jonathan Monteiro, Assistant Professor – Senior Scale
Department of Mechanical and Manufacturing Engineering
Contact Number: +91 96325 19700
Email Id: jonathan.m@manipal.edu

MANIPAL INSTITUTE OF TECHNOLOGY
MANIPAL
(A constituent unit of MAHE, Manipal)

MAY 2021

MANIPAL INSTITUTE OF TECHNOLOGY
MANIPAL
(A constituent unit of MAHE, Manipal)

Manipal
21/05/2021

CERTIFICATE

This is to certify that the project titled **HYDROKINETIC TURBINE DESIGN AND ANALYSIS FOR INDIAN RIVERS** is a record of the bonafide work done by **Abhishek Nain (170909318), Dipayan Maji (170909228), Krishnakanth Mohanta (170909082)** submitted in partial fulfilment of the requirements for the award of the degree of **BACHELOR OF TECHNOLOGY** in **Mechanical Engineering** of Manipal Institute of Technology, Manipal, Karnataka (A constituent unit of Manipal Academy of Higher Education) during the year 2020-2021.

Prof. Jonathan Monteiro — **Project Guide**

Dr Sathya Shankara Sharma — **Head of the department**

CONTENTS

ACKNOWLEDGEMENTS

At the very outset of this report, we would like to extend our sincere & heartfelt obligation towards all the personages who have helped us in this endeavour. Without their active guidance, help, cooperation & encouragement, we would not have made headway in this project.

We pay our deep sense of gratitude to Prof. Jayakrishnan Radhakrishnan, Department of Aeronautical & Automobile Engineering and Prof. Jonathan Monteiro, Department of Mechanical & Manufacturing Engineering, to encourage us to the highest peak and for the valuable guidance and support on completion of this project in its presently.

We want to extend our special thanks to Dr S.S Sharma, HOD, Department of Mechanical & Manufacturing Engineering and Dr Sathish Shenoy B, HOD, Department of Aeronautical & Automobile Engineering for allowing us to do an inter-departmental project.

We extend our gratitude to Manipal Institute of Technology for giving us this opportunity.

We are incredibly thankful to Mr Jousef Murad, Product Marketing Engineer at SimScale, to provide us with premium access to the SimScale software, without which our project would not have been possible.

Last but not least, gratitude goes to all our friends who directly or indirectly helped us complete this project report.

Any omission in this brief acknowledgement does not mean a lack of gratitude.

ABSTRACT

Hydrokinetic Energy is one of the methods that generate energy from sustainable resources. This technology has gained prominence in this era because of its sustainable and environment-friendly nature. A fixed speed straight three-blade horizontal water axis turbine with a radius of 1.4m was designed using an S823 airfoil to harness the hydrokinetic energy from the river current. QBlade was used to optimise the blade geometry. Further, the blade was swept and compared to the straight blade. A computational methodology for the hydrodynamic analysis of horizontal axis hydrokinetic turbine is presented. For that, the CFD method with the shear-stress transport (SST) k-ω model is used to calculate the hydrodynamic moments, estimate the coefficient of performance, and determine the optimal blade parameters for a turbine. The CFD results are then verified using experimental data from previous research papers.

LIST OF NOTATIONS AND ABBREVIATIONS

Notations		Abbreviations	
a	angular induction factor	AoA	angle of attack
a'	axial induction factor	CAD	computer-aided design
A	rotor swept area	CFD	computational fluid dynamics
B	number of blades	HAHT	horizontal axis hydrokinetic turbine
C	blade chord	MRF	multiple reference frame
C_D	drag coefficient	NACA	national advisory committee for aeronautics
C_L	lift coefficient	NREL	national renewable energy laboratory
C_f	skin friction coefficient	RANS	reynolds-averaged navier-stokes
C_p	power coefficient	SST	shear stress transport
P	power	TSR	tip speed ratio
r	radius of blade element or point on blade		
R	blade tip radius		
Re	Reynolds number		
U_t	frictional velocity		
U_∞	free stream velocity		
α	angle of attack		
φ	flow angle of resultant velocity to rotor plane		
λ	tip speed ratio		
λ_r	local speed ratio		
θ_P	section pitch angle		
θ_T	section twist angle		
ρ	water density		
τ_w	wall shear thickness		
ω	angular frequency (rad/s)		

LIST OF FIGURES

LIST OF TABLES

1. Introduction

In the last few years, the scientific community, backed by governments all over the globe, have been working on shifting to renewable sources of energy to reduce the carbon footprint and over-exploitation of fossil fuels. Oceans and rivers constitute a vast, nearly unexploited renewable energy source that can provide enormous amounts of electrical energy. Some forecasts estimate that generation capacity could reach up to 200 GW around the year 2025, and more than 300 hydrokinetic projects are in the pipeline [1].

Hydrokinetic turbines are one of the latest technological trends within hydro-power technology, that captures kinetic energy from the moving streams of rivers and converts them into electrical energy. Earlier hydroelectric dams were used which disturbed the ecosystem where it was built. Unlike the dams, the hydrokinetic turbines can be placed anywhere in the river system, with negligible disturbance to both aquatic as well as the human ecosystem around it.

The energy captured by river streams is better than other modes, from the power generation point of view because of its large power density [2], and the environmental impacts are negligible. The kinetic energy can then be captured by the turbines and utilised to rotate the turbine and subsequently generate electricity. The governing equation in such energy conversion is [3].

$$P = \frac{1}{3}\rho A U^3 C_p \qquad (1)$$

Where P is the power extracted by the turbine (W), ρ is the density of the fluid and, A is the area covered by rotor (m^2), U is the fluid velocity (m/s), and C_p is the power coefficient, a measure of the fluid-dynamic efficiency of the turbine. Therefore, as the generated power is proportional to fluid density, hydrokinetic turbines have a greater energy generation potential compared to wind turbines.

Hydrokinetic turbines have low initial investment as well as maintenance costs, due to which it is cost effective as compared to other modes of energy generation. These turbines give continuous power output which is an added advantage compared to solar power. This kind of hydro power is considered environmentally friendly as water passing through the turbine goes back into

the stream, hence forming no residues. These can be used in remote areas to power villages, and towns without disrupting the environment.

Hydrokinetic turbines have high potential in India due to their compactness and simplicity [4] in the coming years. The blade or the rotor, which converts the kinetic energy of the wind or water current into mechanical energy, is an essential component of a turbine system. The rotor's design is considered a primary challenge from both a hydrodynamic and economic standpoint. The performance of the rotor is a function of the number of blades, the axis of turbine, tip speed ratio, type of airfoil, chord length, and twist and distribution along the blade span [5], and all of these parameters were optimised to utilise maximum power from the free stream of the river.

This project work is looking forward to designing and analysing a floating water turbine for the Indian rivers. For the study, velocity in the year 2013-14 at three sites - Haridwar, Bahadrabad, Roorkee of River Ganga was considered [6]. The seasonal variation of velocity at these three sites are shown in Table 1

Table 1: Seasonal variation of velocity for River Ganga

Month	Site-1: Haridwar	Site-2: Bahadrabad	Site-3: Roorkee
Oct	1.59	1.61	1.62
Nov	1.32	1.4	1.3
Dec	1.01	0.97	0.99
Jan	1.27	1.29	1.17
Feb	1.47	1.51	1.42
Mar	1.43	1.27	1.36
Apr	1.51	1.56	1.52
May	1.23	1.23	1.16
Jun	1.46	1.36	1.47
Jul	1.63	1.64	1.58
Aug	1.28	1.34	1.25
Sep	1.25	1.04	1.25

Velocity at three sites varied from 0.97 m/s - 1.63 m/s. It was attempted to maximise the power coefficient around 1.4 m/s, which is the river's velocity for the maximum period in a year.

2. Importance of proposed work

The floating water turbine attempts to make renewable source of energy more feasible for use. This project aims to design and optimise the turbine design so as to achieve better efficiency than the current designs available in the market to promote use of wide use of hydrokinetic turbines for energy generation.

India being the land of rivers, hydrokinetic turbines have a broad scope for development in this country. Its Megawatts of energy going without being utilised each year. Starting a project aiming on utilisation of hydropower from the rivers in the country has never been easy as it was earlier associated with dams.

Construction of Dams have always posed lot of problems to the ecology and ecosystem around the place of construction. The project encourages a shift to floating water turbines which can be installed anywhere along the river, even in shallow regions, without affecting any land or marine ecosystem.

Hence this project looks forward to bringing a change and encourages the use of renewable sources of energy and improve the current state use of hydrokinetic turbines to make it more feasible to be used throughout the country and abroad.

3. Literature Review

Sustainable management of water resources requires that the long-term future, as well as present, needs are considered in a balanced way. According to UNESCO (1999), sustainable water resource systems are those designed and managed to fully contribute to the objectives of society, now and in the future, while maintaining their ecological environmental and hydrological integrity [19].

The current market trend was studied. Extracting power of a running river or a stream to convert it into electricity has been a topic of interest for many researchers as well as manufacturers. The technology of small-scale hydro power is trending, and different concepts have been developed and applied [20].

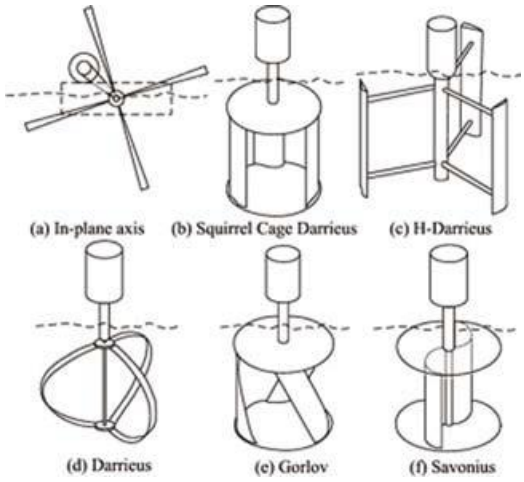

Figure 1: Different types of blade designs

Designs for hydrokinetic turbines were studied. The Darrieus type and Savonius type were the most effective among vertical axis hydrokinetic turbine. But considering the seasonal fluctuation of depth of the rivers, vertical axis may pose problems like space constraints. The Gorlov Turbine suffers from uneven force distribution along the blade whereas Darrieus type has vibrations as a major drawback. Also, the energy density and the efficiency of Vertical Axis turbines were lower compared to horizontal axis hydrokinetic turbines. Hence Horizontal Axis Hydrokinetic Turbine (HAHT) was preferred and further studied for design optimisation.

River data was analysed. Seasonal variation of the river Ganga was studied at 3 locations. The design has to be done considering the seasonal variation in speed to capture and convert maximum energy throughout the year

4. Problem Statement

To design and analyse a floating water turbine to capture energy from the flowing water of a river system and convert it into usable energy and to optimise design so as to produce a more efficient hydrokinetic turbine than the designs currently in use.

5. Objective

The objectives of the project are:

- Determining Indian rivers flow pattern and its challenges:
- Designing water turbine through CAD designs
- Analysis of turbine through simulations
- Comparison of new design with existing models in the market

6. Design of Straight Blade Turbine

6.1. Design: Selection of Airfoil for Turbine

The blade design's main attributes are the airfoil, section pitch angle, chord length, and tip-speed ratio. The mentioned parameters are optimised to extract the maximum energy from the flow.

NACA 6 Series and NERL airfoil's geometry are readily available and widely used in wind and water turbines; therefore, they were our primary choices. After evaluation, S823 airfoil was selected for our blade design because it was relatively thicker than NACA airfoils with a max thickness of 21.2% at 24.3% chord [7], thus being less sensitive to surface roughness which is an essential trait for underwater turbines as they are more likely to be subjected to debris and foreign object damage.

S823 was then analysed using XFLOIR and the results showed that max C_L/C_D of the airfoil was produced at an angle of attack of 6°.

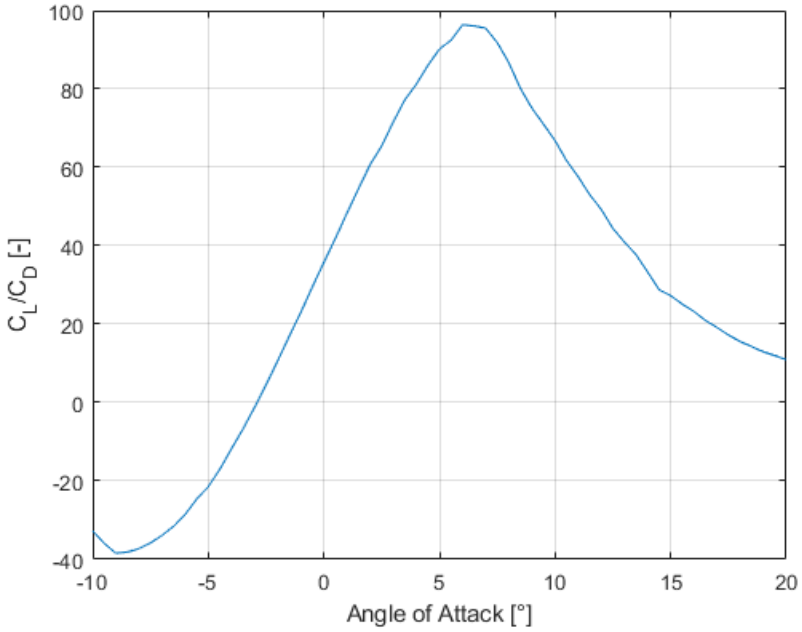

Figure 2: C_L/C_D vs AoA for S823 Airfoil

6.2. Calculation of Blade Parameters

The tip speed ratio is defined as the ratio of the speed of tips of the turbine blade to the free stream velocity; there are numerous models to decide upon an optimum TSR. We are designing a turbine with constant speed, which means that TSR will change with respect to the flow velocity. A fixed-speed turbine is designed because in the case of a variable-speed turbine, as the stream velocity decreases, to maintain constant TSR, the turbine has to rotate at high angular velocities, which may cause problems like cavitation, excessive vibration, and noise. For a three-blade Turbine, optimum TSR should lie between 6 to 8 [8]. For the purpose of calculations, TSR 6 was chosen.

The calculation for chord length and angle of relative wind was done according to Blade Elements Theory and the following assumptions are made:

- There is no aerodynamic interaction between elements (thus, no radial flow)
- The forces on the blades are determined solely by the lift and drag characters of the airfoil shape of the blades.

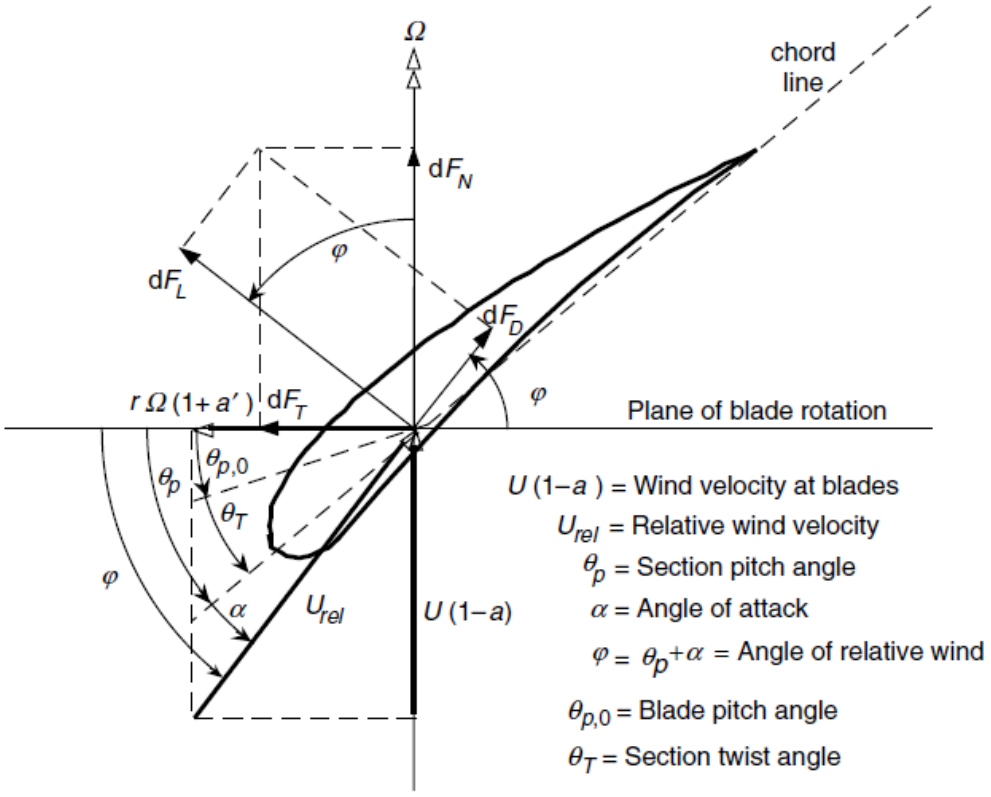

Figure 3: Blade nomenclature for a horizontal axis Turbine

Considering the most ideal case i.e., Betz Limit, where angular induction factor (a') = 0 and Axial Induction factor (a) = 1/3 we get the following formula [9]:

$$\text{Chord Length, } c = \frac{8\pi r \sin(\phi)}{3BC_L\lambda_r} \tag{2}$$

$$\text{Angle of relative wind, } \phi = tan^{-1}\left(\frac{2}{3\lambda_r}\right) \tag{3}$$

$$\text{Section pitch angle (Twist), } \theta_p = \phi - \alpha \tag{4}$$

6.3. Optimisation of Blade Parameter via QBlade

QBlade is an open-source, cross-platform simulation software for wind turbine blade design and aerodynamic simulation. The above calculations were imported to QBlade, and Horizontal Turbine's Twist was optimised for optimal Lift/Drag Ratio, and the Chord was optimised according to Betz Theory.

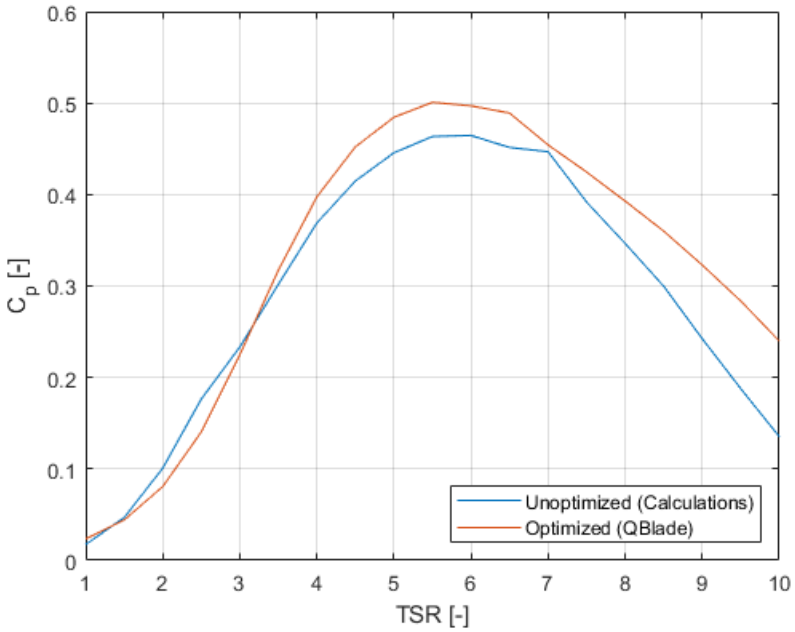

Figure 4: Cp vs TSR Graph before and after QBlade Optimization

It can be seen that our assumption that maximum Cp will lie around TSR 6 was correct. Moreover, there is an increase of 8.06% in Cp at TSR 5.5 and a 6.09% increase at TSR 6 because of QBlade optimisation.

6.4. Geometry

The blade geometry was optimised using QBlade. Initial unoptimised geometry details of the Turbine blade are as follows:

Table 2: Unoptimized Turbine Geometry Details

Radius (m)	Chord Length(m)	Twist (°)
0.32	0.395	41.513
0.44	0.258	22.555
0.56	0.185	13.823
0.68	0.142	9.024
0.8	0.115	6.029
0.92	0.097	3.991
1.04	0.083	2.519
1.16	0.073	1.407
1.28	0.065	0.538
1.4	0.059	-0.160

The optimised geometry of the blade is as follows:

Table 3: Geometry details of Optimised Blade

Radius (m)	Chord Length(m)	Twist (°)
0.32	0.282	19.920
0.44	0.215	13.470
0.56	0.172	9.520
0.68	0.144	6.890
0.8	0.123	5.000
0.92	0.107	3.600
1.04	0.095	2.510
1.16	0.086	1.640
1.28	0.078	0.930
1.4	0.071	0.340

The coordinates of the blade were imported to CATIA V5 and the geometry was modelled with a hub radius of 0.2m. At the root of the blade a circular airfoil with a diameter of 0.1m is used.

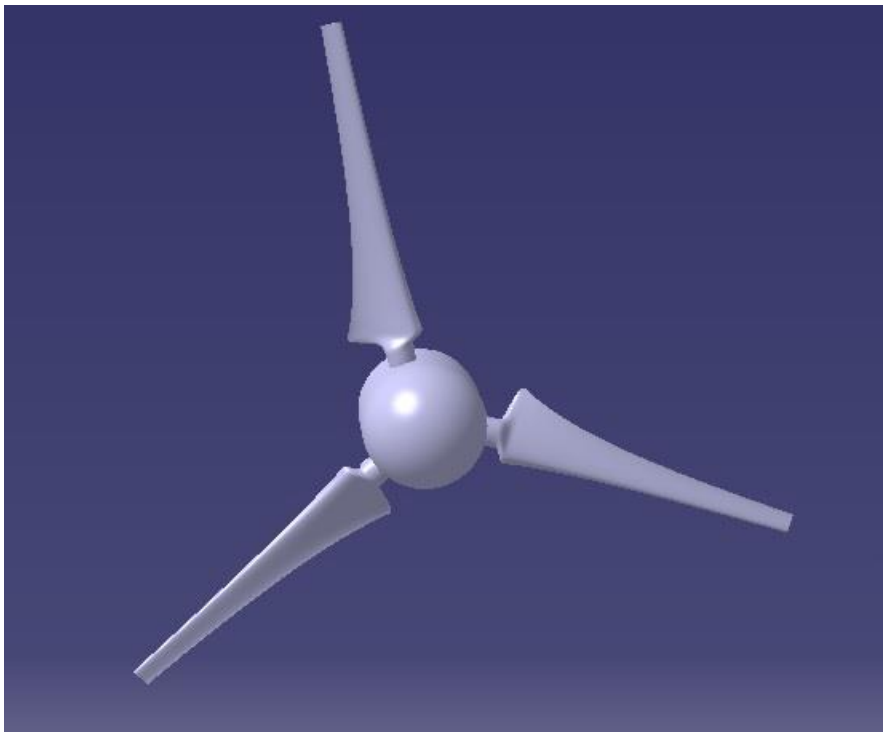

Figure 5: 3D CAD of Straight Blade Turbine

6.5. CFD Analysis of Straight Blade Turbine

The evaluation of the performance of the hydrokinetic turbine was done by running CFD simulations in SimScale. Performance of a turbine Cp can be quickly and fairly accurately determined using either a steady-state or a transient simulation. However, a quasistatic approach is numerically less expensive, and it can be applied rapidly to determine the general turbine performance indicator [10].

The SST k- ω turbulence model [11] is a two-equation eddy-viscosity model which has become very popular. The shear stress transport (SST) formulation combines the best of two worlds. The use of a k-ω formulation in the inner parts of the boundary layer makes the model directly usable all the way down to the wall through the viscous sub-layer, hence the SST k- ω model can be used as a Low-Re turbulence model without any extra damping functions. The SST formulation also switches to a k-ε behaviour in the free-stream and thereby avoids the common k- ω problem that the model is too

sensitive to the inlet free-stream turbulence properties [12] k- ω turbulence model belongs to the Reynolds-averaged Navier-Stokes (RANS) family of turbulence models where all the effects of turbulence are modelled. The equations of the SST k- ω model can be written as follows [13].

$$\underbrace{\frac{\partial(\rho k)}{\partial t}}_{\text{rate of change of k}} + \underbrace{\operatorname{div}(\rho k\mathbf{U})}_{\text{transport of } k \text{ by convection}} = \underbrace{\operatorname{div}[(\mu + \frac{\mu_t}{\sigma_k})\operatorname{grad}(k)]}_{\text{transport of } k \text{ by turbulent diffusion}} + \underbrace{(2\mu S_{ij}.S_{ij} - \frac{2}{3}\rho k\frac{\partial U_i}{\partial x_j}\delta_{ij})}_{\text{production rate of } k} - \underbrace{\beta_1\rho k\omega}_{\text{dissipation rate of } k} \quad (5)$$

The equation for ω is-

$$\underbrace{\frac{\partial(\rho\omega)}{\partial t}}_{\text{rate of change of } \omega} + \underbrace{\operatorname{div}(\rho\omega\mathbf{U})}_{\text{transport of } \omega \text{ by convection}} = \underbrace{\operatorname{div}[(\mu + \frac{\mu_t}{\sigma_{\omega,1}})\operatorname{grad}(\omega)]}_{\text{transport of } \omega \text{ by turbulent diffusion}} + \underbrace{\gamma_2(2\rho S_{ij}.S_{ij} - \frac{2}{3}\rho\omega\frac{\partial U_i}{\partial x_j}\delta_{ij})}_{\text{production rate of } \omega} - \underbrace{\beta_2\rho\omega^2}_{\text{dissipation rate of } \omega} + \underbrace{2\frac{\rho}{\sigma_{\omega,2}\omega}\frac{\partial k}{\partial x_k}\frac{\partial \omega}{\partial x_k}}_{\text{cross diffusion term}} \quad (6)$$

The Multiple Reference Frame (MRF) incompressible flow was considered. The MRF rotating zone is a steady-state approximation of the transient rotating motion at an instance of time. Therefore, the mesh/body is not physically rotated. This approach uses a rotating frame of reference that modifies the governing equations in the rotating zone. Additional source terms that incorporate forces in the rotating reference frame are taken into account. These simulate a rotation effect in the flow [14]. Performing MRF simulations is computationally much less demanding than transient modelling.

A cuboidal bounding box was taken with both width and height equal to 5.5 D. The velocity inlet was set to 4.6D upstream and the pressure outlet at 8.6D downstream. Meshing was done by giving appropriate surface and region refinement.

Y+ is a non-dimensional distance from the wall to the mesh node. To capture the viscous sublayer, the desired y+ value should be less than 5, in this region it is assumed

that the shear stress is approximately constant and equal to the wall shear stress τ_w throughout the layer [13]. Accordingly, the first layer thickness was calculated with the help of following formula [15].

$$\Delta y_1 = \frac{y+\ \mu}{\rho\ .\ U_t} \qquad (7)$$

Where U_t is the frictional velocity and is defined as,

$$U_t = \sqrt{\frac{\tau_w}{\rho}} \qquad (8)$$

The wall shear thickness, τ_w can be calculated from skin friction coefficient, C_f as follows,

$$\tau_w = \frac{1}{2} C_f . \rho . U^2 \qquad (9)$$

The skin friction coefficient was calculated using Schlichting skin-friction correlation which is valid for Re < 10^9

$$C_f = [2 \log_{10} R_e - .65]^{-2.3} \qquad (10)$$

Simulation was run at velocity 1.4 m/s with different mesh sizes to ensure grid-independence of results. Moments and forces were studied with three different mesh configurations with 7.2, 11.2, and 14.6 million cells, respectively. In all three cases, the hydrodynamic moments and forces came out to be approximately the same, with 1 to 2% error. Table 4 shows the values of moments for different mesh sizes.

Table 4: Value of moments at different Mesh size

Mesh Size	Pressure Moment	Viscous Moment	Net Moment
7.2 Million	674.49	-44.61	629.88
11.2 Million	654.74	-44.41	610.29
14.6 Million	655.81	-43.11	612.7

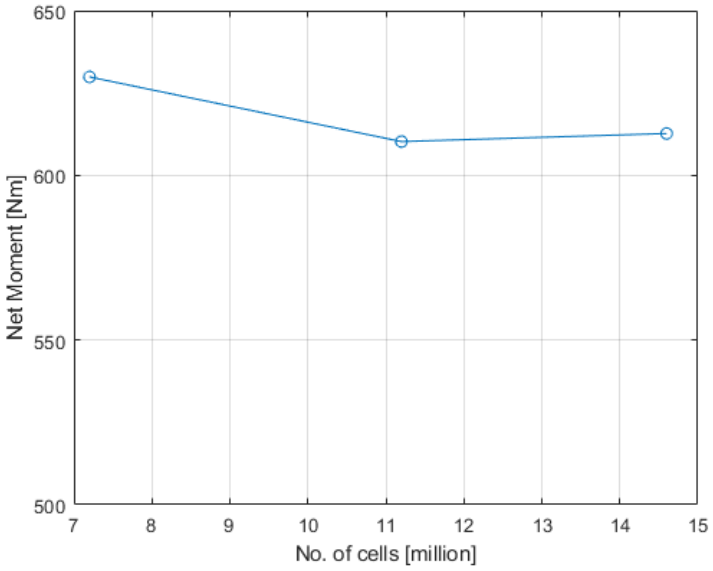

Figure 6: Net moment at different mesh size

Net moment for different mesh sizes is shown in the plot in Figure 6. To maintain a balance between accuracy and computation time, it was decided to go ahead with the mesh consisting 11.2M cells. The mesh parameters are shown in Table 5. The pictorial representation of the bounding box is shown in Figure 7.

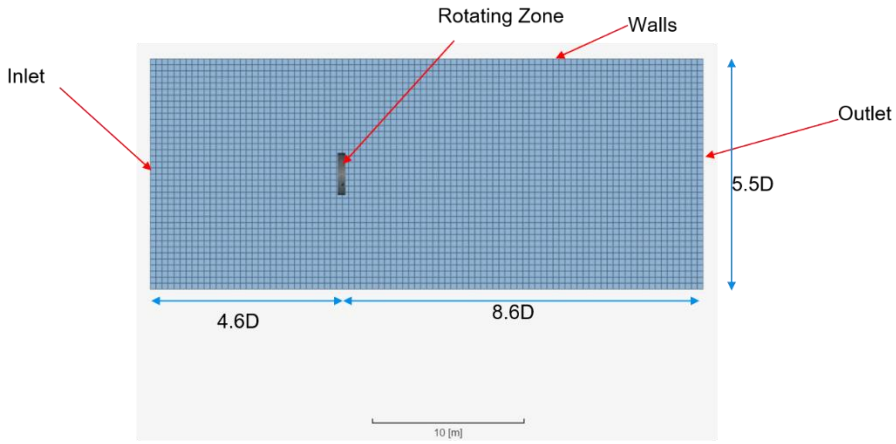

Figure 7: Bounding Box Dimensions (Diameter of Turbine D =2.8 m)

Table 5: Mesh Parameters

Bounding Box Dimension	15.4m x 15.4m x 36.96m
No. of cells	11.2M
No. of nodes	13.2M
No. of inflation layers	15
Inflation Expansion Ratio	1.3
First Layer Thickness	0.01 mm
Turbulence intensity	5%

Surface Mesh for the straight blade turbine is shown in Figure 8. Mesh at 50% span of the blade is shown in Figure 9.

Figure 8: Surface Mesh of Straight Blade Turbine

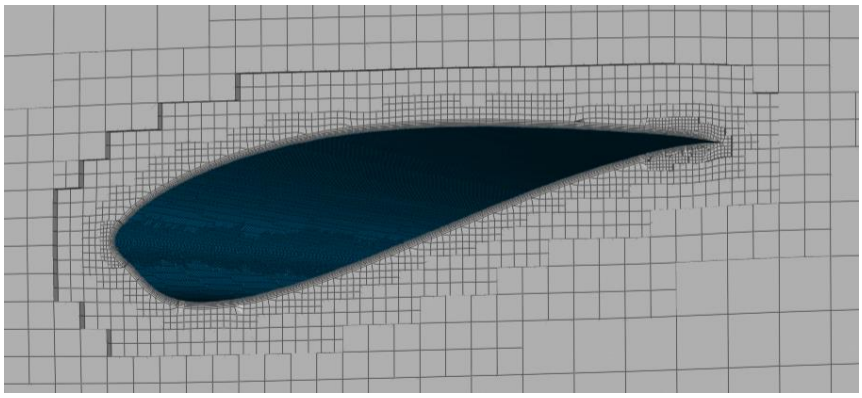

Figure 9: Mesh Clip at 50% span of blade

Since the design is for a fixed-speed turbine, the TSR will be a function of free stream velocity and was calculated with the help of following formula.

$$TSR = \frac{\omega . R}{U_\infty} \qquad (11)$$

Maximum efficiency according to QBlade lied around TSR 6, therefore TSR 6 was maintained at the mean flow velocity of 1.4 m/s. The boundary conditions used are shown in Table 6.

Table 6: Boundary Conditions

Velocity Inlet	1 to 2 m/s
Pressure Outlet	0 Gauge Pressure
Bounding box side walls	Slip
Turbine walls	No-Slip
Rotating Zone	6 rad/s Rotational Velocity

The CFD analysis shows the y+ value distribution across the blade. The placement of the first node from the near wall inflation mesh is crucial in CFD analysis. Y+ is the non-dimensional distance from the wall to the mesh node. Y+ value of less than 3 was maintained throughout the blade profile to ensure capturing of the wall functions, and accordingly the first layer thickness for the inflation layer was decided.

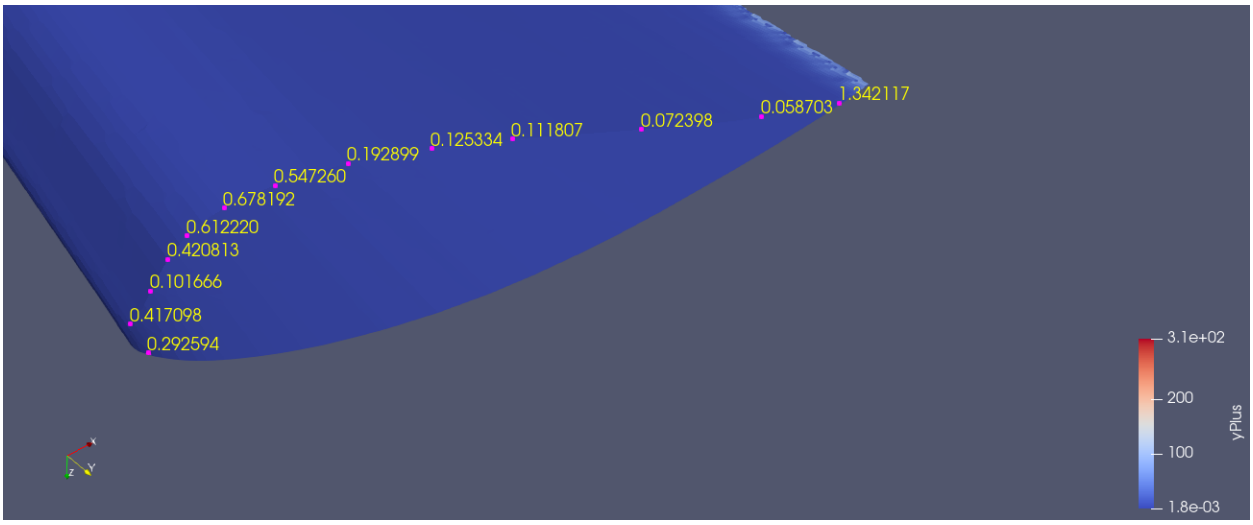

Figure 10: Y+ value distribution on the blade profile

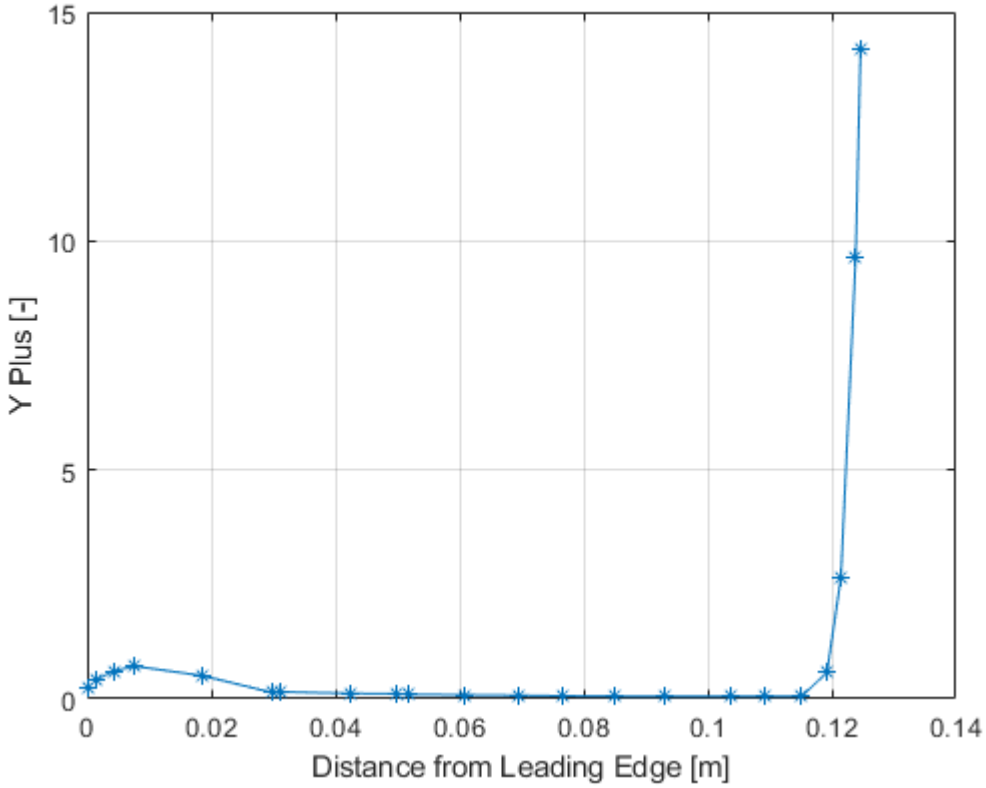

Figure 11: Graph of y+ value vs Distance from Leading Edge

The simulation was run for 2000 time-steps to ensure the convergence of the solution.

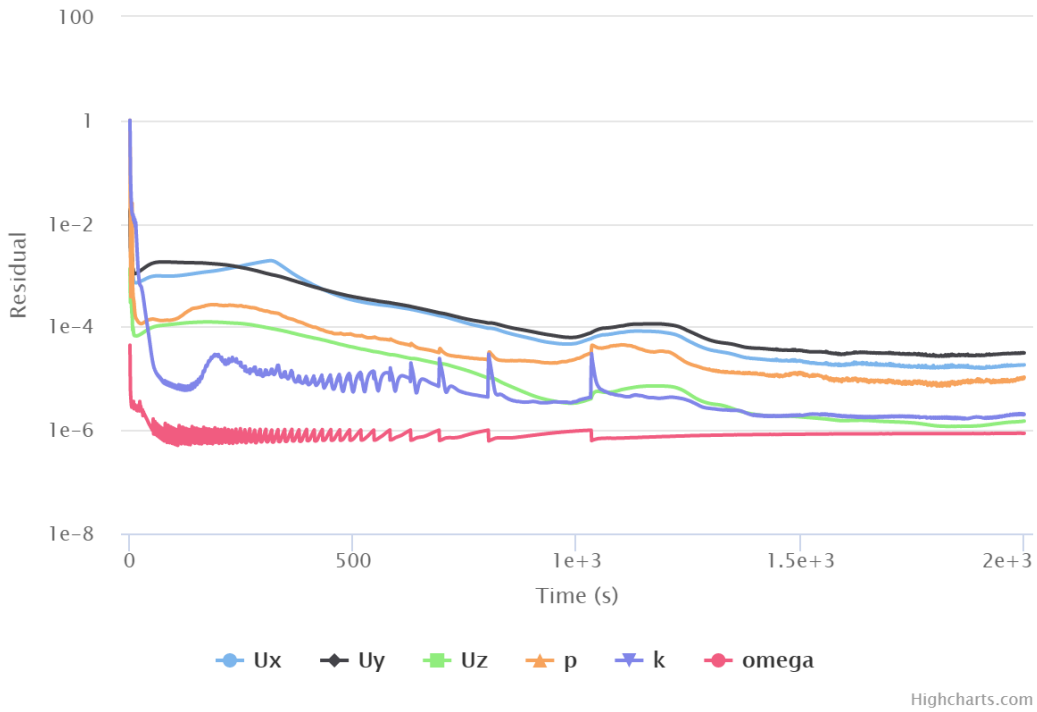

Figure 12: Residual Convergence Plot for inlet velocity = 1.4m/s

6.6. Power Calculations for Straight Blade Turbine

Power = (Pressure Moment + Viscous Moment) *Rotational Velocity (12)

Table 7: Power Calculation for Straight Blade Turbine

Velocity	TSR	Pressure Moment	Viscous Moment	Power Produced
1	8.40	180.92	-45.56	812.22
1.2	7.00	403.19	-44.71	2150.91
1.3	6.46	524.31	-44.53	2878.72
1.4	6.00	654.74	-44.49	3661.54
1.5	5.60	797.45	-44.62	4516.99
1.6	5.25	945.81	-44.63	5407.12
1.8	4.67	1278.07	-43.60	7406.78
2	4.20	1549.45	-40.86	9051.52

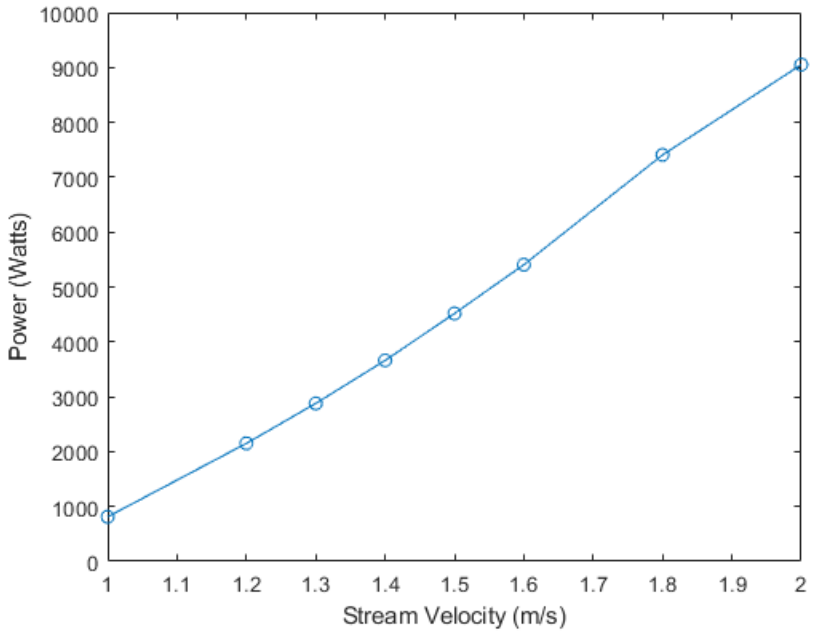

Figure 13: Power vs Velocity Graph of Straight Blade Turbine

The power coefficient was calculated according to the formula:

$$C_p = \frac{Power}{\frac{1}{2}.\rho.A.v^3} \qquad (13)$$

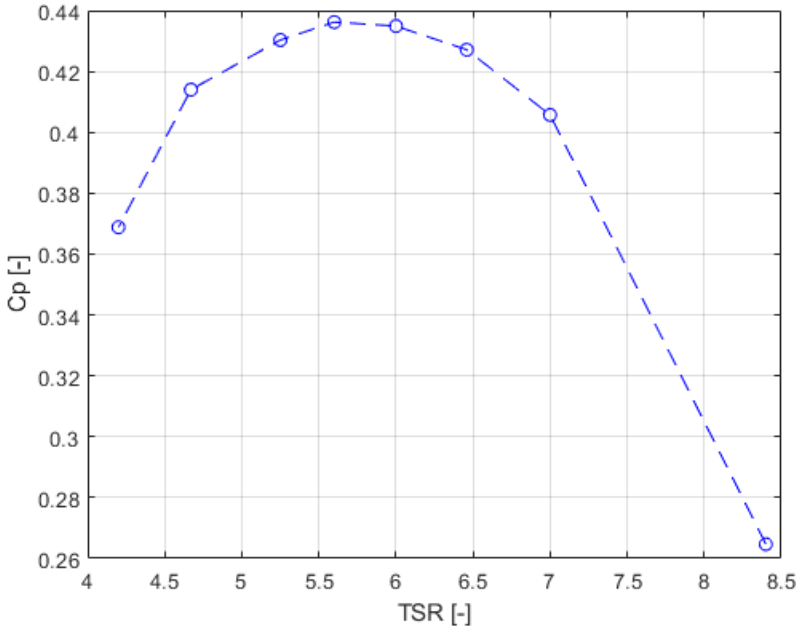

Figure 14: Cp of Straight Blade Turbine

Further the results from CFD were compared to QBlade results. As mathematical formulations which is used in QBlade is based on Blade Element Momentum method [16], while comparing with CFD results viscous moment was ignored. The comparison is shown in Figure 15.

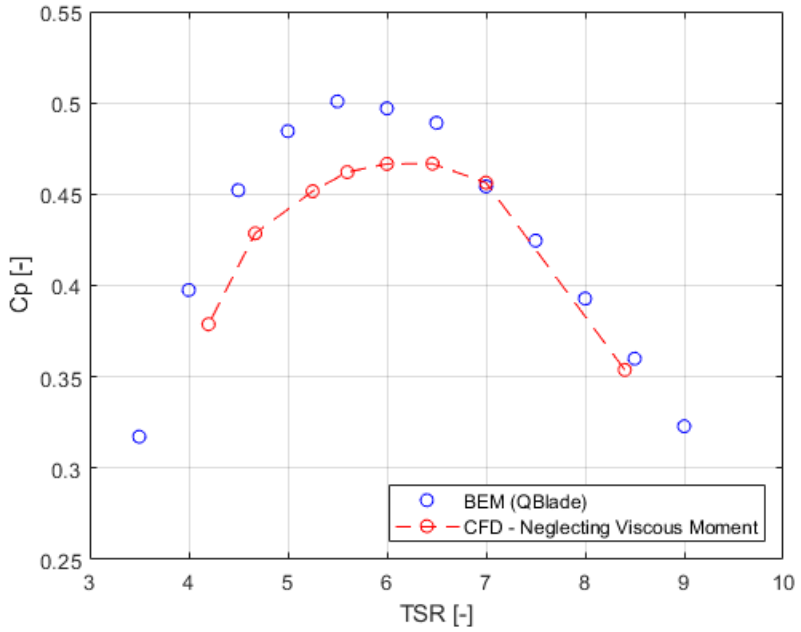

Figure 15: Cp vs TSR Graph - Comparison with QBlade

As expected CFD results were lower than QBlade data, these losses can be attributed to losses due to hub and other assumptions, as BEM is an ideal condition.

7. Design Optimisation using Sweep Curving

7.1. Sweep Curving of Straight Blade

In Figure 16, on the stacking line of swept blade, three points from left to right are point A (x_A, y_A), point B (x_B, y_B), point C (x_C, y_C). For the points A, B, C, the equation of stacking line of swept blade can be deduced by using Lagrange interpolation method.

$$y = \frac{(x - x_A)(x - x_C)}{(x_B - x_A)(x_B - x_C)} . y_B + \frac{(x - x_A)(x - x_B)}{(x_C - x_A)(x_C - x_B)} . y_C \qquad (14)$$

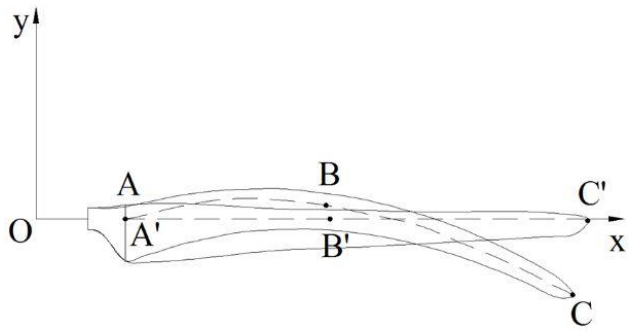

Figure 16: Sketch map of swept and straight blade

In order to ensure the optimised blade has the same swept area with the straight blade, the coordinates of point C should meet $x_C^2 + y_C^2 = R^2$. Where R is a straight blade radius, and x_C can be expressed by $x_C = \sqrt{R^2 - y_C^2}$. Point A (xA, yA) are determined by hub radius. The other three parameters x_B, y_B and y_C need to be optimised and then obtain the equation of stack line of swept blade.

An iterative approach was followed to sweep the blade, where the points of curve followed by the blade was interpolated using Lagrange Interpolation method to optimise the swept blade for max Cp. The final equation of the swept blade curve is

$$y = -0.091(x - 0.323)(x - 1.199) - 0.070(x - 0.323)(x - 0.586) \quad (15)$$

where x ranges from 0.323 m to 1.4 m and y is the lateral displacement of the blade section at corresponding x. No other parameters such as airfoil chord length or twist was changed when compared to the straight blade. It was made sure that the radius of swept blade turbine is also maintained at 1.4 m with a hub of 0.2 m. Figure 17 shows the CAD of the turbine after curve sweeping.

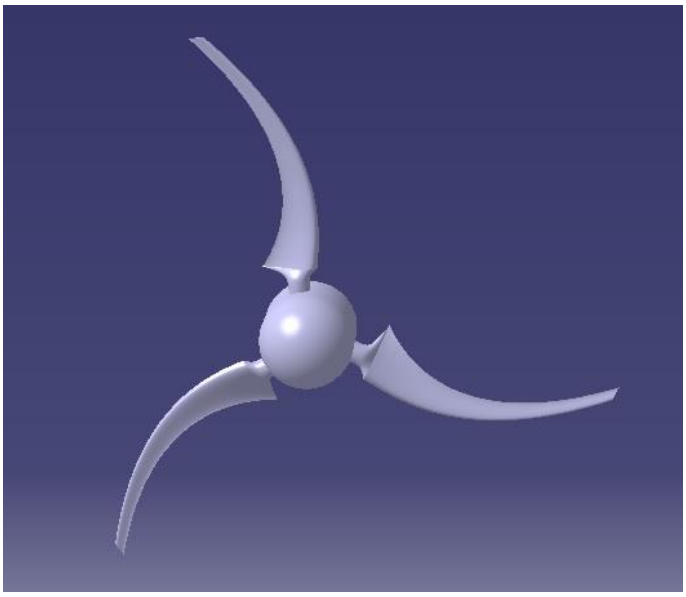

Figure 17: 3D CAD of Swept Blade Turbine

7.2. CFD Analysis of Swept Blade Turbine

The design was then set for CFD simulations keeping the same mesh settings and boundary conditions. The mesh generated had 10.9M cells. The surface mesh of the turbine is shown in Figure 18.

Figure 18: Surface Mesh of Swept Blade

The rotation velocity was also kept same and maintained at 6 rad/s. Power was calculated for the turbine and is shown in Table 8.

Velocity	Pressure Moment	Viscous Moment	Power Produced	Cp
1	216.50	-42.53	1043.77	0.340
1.2	420.69	-42.11	2271.47	0.428
1.3	538.05	-42.07	2975.85	0.441
1.4	665.20	-42.23	3737.77	0.444
1.5	805.19	-42.48	4576.22	0.442
1.6	952.65	-42.66	5459.89	0.434
1.8	1276.40	-42.05	7406.12	0.414
2	1601.25	-40.43	9364.92	0.382

Table 8: Power and Cp Calculation for Swept Blade Turbine

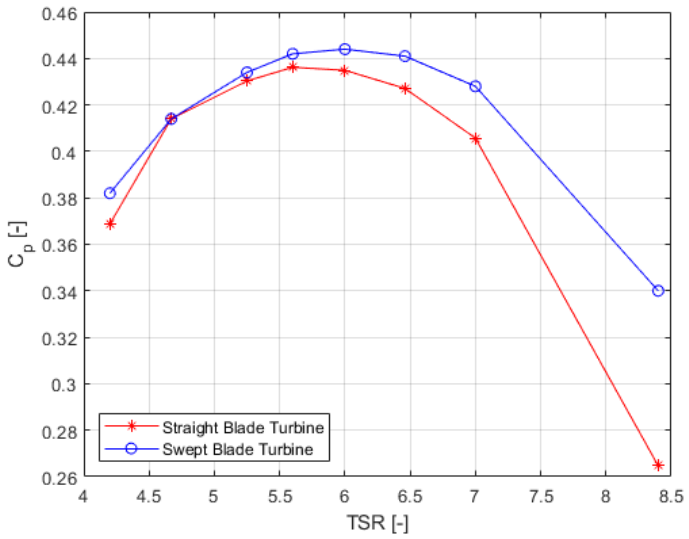

Figure 19: Comparison of Cp of Straight Blade Turbine and Swept Blade Turbine

In Figure 19 it can be seen that the Swept Blade Turbine yields a higher efficiency and is proved to be aerodynamically better when compared to the Straight Blade Turbine. Maximum increase in the power coefficient is 28.45% at TSR 8.4, and the average increase in Cp is 5.63%. The possible reason for the increase in power can be because the streamline on the suction of a swept blade is outward oblique, which in turn may benefit the out torque of the swept blade and lower speeds (high TSR) [17].

8. Validation of CFD Model

To ensure the reliability of the results of this study, it was validated with the experimental data from a previous turbine [18]. A 3 blade Horizontal Axis Turbine with 350 mm rotor radius composed of NACA 63418 airfoils was studied for TSR varying from 3 to 9 and the geometry details are given in Table 9. The experimental model is shown in Figure 20.

Figure 20: Experimental Model

Table 9: Geometric Details of Turbine for Validation

Airfoil Profile	NACA 63418
Rotor Radius	350 mm
Hub Radius	45 mm
Rotor Depth	1000 mm
Nacelle Length	720 mm

Table 10: Blade Parameter of turbine for Validation

r/R	c/R	Pitch (degree)
0.1333	0.0567	29.5672
0.15	0.0567	29.5672
0.155	0.0567	29.5672
0.1983	0.1521	25.6273
0.2417	0.2474	22.1491
0.285	0.2375	19.3031
0.3283	0.2259	16.9737
0.3717	0.2141	15.0538
0.415	0.2029	13.4572
0.4583	0.1925	12.1169
0.5017	0.1829	10.9815
0.545	0.1743	10.0114
0.5883	0.1665	9.1761
0.6317	0.1594	8.4516
0.675	0.1529	7.8191
0.7183	0.1471	7.2638
0.7617	0.1418	6.7735
0.805	0.137	6.3387
0.8483	0.1325	5.9514
0.8917	0.1285	5.605
0.935	0.1247	5.2941
0.9783	0.1213	5.0143
1	0.0655	4.8743

Table 10 shows the blade parameters of the turbine used for validation. A 3D geometry was made considering all the above geometry, the missing parameters such as distance of nacelle from the blades was approximately assumed and the final CAD was made through CATIA (Figure 21). The surface mesh is shown in Figure 22.

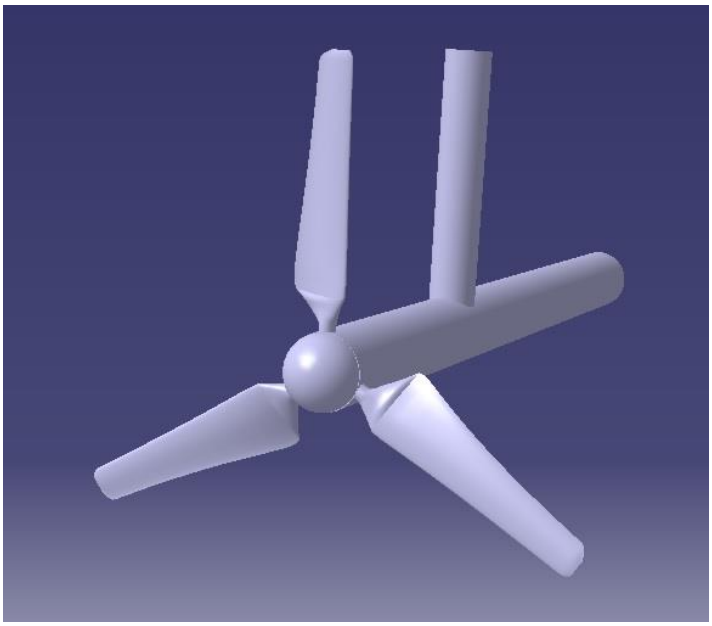

Figure 21: 3D CAD of Turbine for Validation

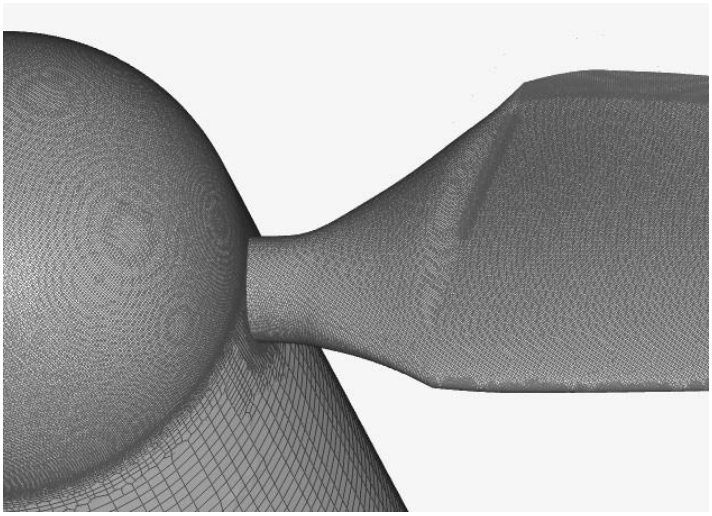

Figure 22: Surface Mesh at Blade Root of Turbine for Validation

The velocity inlet was subject to a constant velocity of 1 m/s. Omega was calculated for various TSR ranging from 3 to 9, and simulation was run.

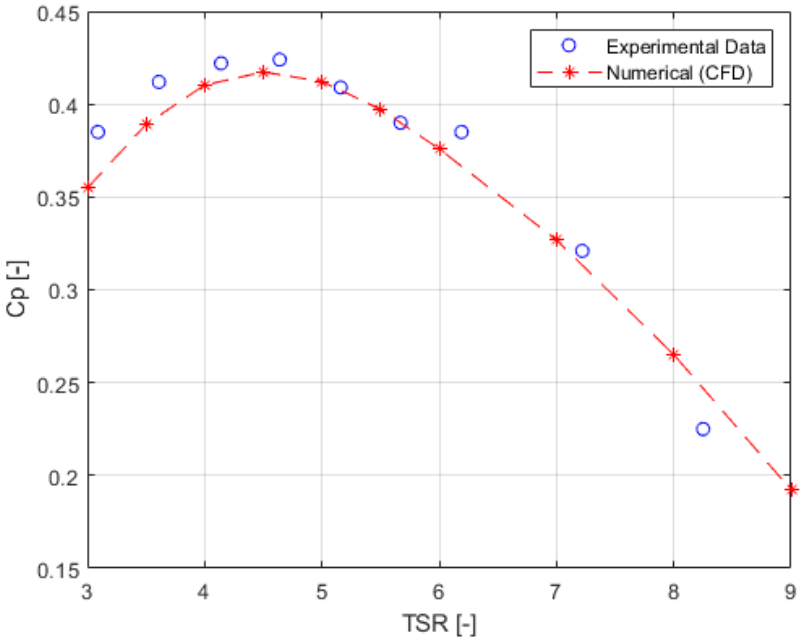

Figure 23: Cp comparison of Numerical and Experimental Data

When comparing our CFD results with the actual experimental setup results (Figure 23), we observed a mean percent error of 1.377% and a mean absolute error of 0.0138 in the values which is well within the acceptable range, thus validating our CFD model.

9. Conclusions

It can be seen that there is a significant increase of power coefficient for higher values of TSR in case of a Swept Blade (refer Figure 24). This will help us extract more power when the flow exhibits lower velocity, therefore proving ideal with respect to our application. The constant rotational speed will help in easier designing of generator and will require no extra mechanism for stall or pitch control (Required in case of a variable speed rotor).

Design of a water turbine suitable for Indian rivers is successfully done and yields a better power output compared to the current market trend.

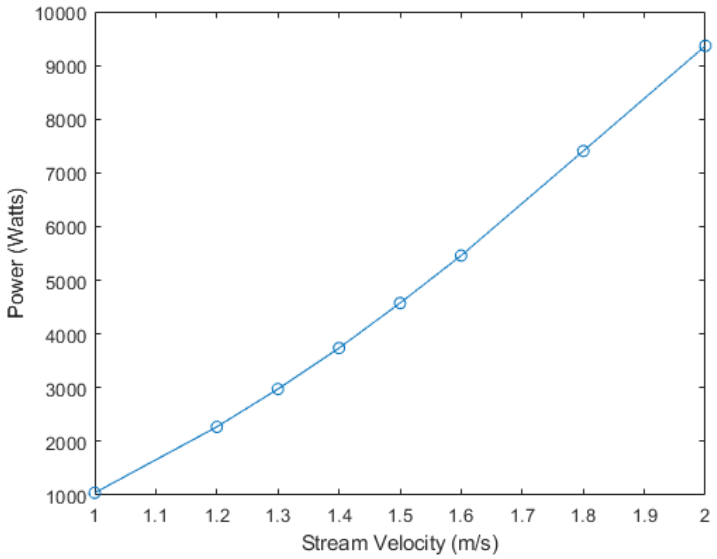

Figure 24: Power vs Velocity Graph of Swept Blade Turbine

The turbine can produce 1 kW at a free stream flow velocity of 1 m/s and can produce up to 9.3 kW at 2 m/s stream velocity.

10. References

1. M. Guney, K. Kaygusuz, Hydrokinetic energy conversion systems: A technology status review, Renewable and Sustainable Energy Reviews 14 (9) (2010) 2996{3004. doi:10.1016/j.rser.2010.06.016.
2. B. E. Layton, A comparison of energy densities of prevalent energy sources in units of joules per cubic meter, International Journal of Green Energy 5 (6) (2008) 438-455. doi:10.1080/15435070802498036.
3. M. Khan, M. Iqbal, J. Quaicoe, River current energy conversion systems: Progress, prospects and challenges, Renewable and Sustainable Energy Reviews 12 (8) (2008) 2177-2193. doi:10.1016/j.rser.2007.04.016.
4. B. Kirke, Hydrokinetic and ultra-low head turbines in rivers: A reality check, Energy for Sustainable Development 52 (2019) 1-10. doi:10.1016/j.esd.2019.06.002.
5. S. Hazim, A. EL Ouatouati, M. T. Janan, Modeling approach for hydrokinetic turbine, 2016 International Renewable and Sustainable Energy Conference (IRSEC) (2016). doi:10.1109/irsec.2016.7983893.
6. G. Matta, A. Kumar, S. Srivastava, V. Singh, G. Dhingra, Impact assessment on water quality of ganga canal system in himalayan region, International Journal of Scientific and Engineering Research 6 (2010) 1524 - 1531.
7. D. M. Somers, S822 and s823 airfoils: October 1992-December 1993 (2005). doi:10.2172/15011666.
8. N. Cetin, M. Yurdusev, R. Ata, A. Ozdamar, Assessment of optimum tip speed ratio of wind turbines, Mathematical and Computational Applications 10 (1) (2005) 147-154. doi:10.3390/mca10010147.
9. J. F. Manwell, M. G. J. G., A. L. Rogers, Wind energy explained, John Wiley & Sons, 2002.
10. T. Leroux, N. Osbourne, D. Groulx, Numerical study into horizontal tidal turbine wake velocity deficit: Quasi-steady state and transient approaches, Ocean Engineering 181 (2019) 240{251. doi:10.1016/j.oceaneng.2019.04.019.

11. F. Menter, Zonal two equation k-w turbulence models for aerodynamic flows, 23rd Fluid Dynamics, Plasmadynamics, and Lasers Conference (1993). doi:10.2514/6.1993-2906.
12. Sst k-omega model URL https://www.cfd-online.com/Wiki/SST_k-omega_model
13. H. Versteeg, W. Malalasekera, An Introduction to Computational Fluid Dynamics, Prentice Hall, 2007.
14. Rotating zones: Advanced concepts: Simscale documentation (10 2020). URL https://www.simscale.com/docs/simulation-setup/advanced-concepts/rotating-zones/
15. Y plus wall distance estimation. URL https://www.cfdonline.com/Wiki/Y_plus_wall_distance_estimation
16. D. Marten, J. Wendler (01 2013).URL http://qblade.org/project_images/files/guidelines_v06.pdf
17. H. M. Zuo, C. Liu, H. Yang, F. Wang, Numerical study on the effect of swept blade on the aerodynamic performance of wind turbine at high tip speed ratio, Journal of Physics: Conference Series 753 (2016) 102010. doi:10.1088/1742-6596/753/10/102010
18. P. Mycek, B. Gaurier, G. Germain, G. Pinon, E. Rivoalen, Experimental study of the turbulence intensity effects on marine current turbines behaviour. part i: One single turbine, Renewable Energy 66 (2014) 729-746. doi:10.1016/j.renene.2013.12.036
19. Sharad K. Jain & Pradeep Kumar (2014) Environmental flows in India: towards sustainable water management, Hydrological Sciences Journal, 59:3-4, 751-769, DOI: 10.1080/02626667.2014.896996
20. Small-scale Water Current Turbines for River Applications: Zero Emission Resource Organization

Plagiarism Report

plgm1

ORIGINALITY REPORT

10%	8%	8%	6%
SIMILARITY INDEX	INTERNET SOURCES	PUBLICATIONS	STUDENT PAPERS

PRIMARY SOURCES

1	www.cfd-online.com Internet Source	3%
2	www.simscale.com Internet Source	2%
3	E. Chica, F. Pérez, A. Rubio-Clemente, S. Agudelo. "Design of a hydrokinetic turbine", WITPRESS LTD., 2015 Publication	1%
4	link.springer.com Internet Source	1%
5	www.coursehero.com Internet Source	1%
6	S. Laín, L. T. Contreras, O. López. "A review on computational fluid dynamics modeling and simulation of horizontal axis hydrokinetic turbines", Journal of the Brazilian Society of Mechanical Sciences and Engineering, 2019 Publication	1%
7	Submitted to University of Lancaster Student Paper	1%